 ICCES, vol.10, no.2, pp.77-86

Chaotic Mixing in a Microfluidic Device

Chih-Chang Chang, Ruey-Jen Yang[1]

Summary

This paper presents a theoretical investigation into chaotic mixing in low Reynolds number electro-osmotic flows. In this mixing system, the primary flow is the plug-like electro-osmotic flow contributed by the permanent surface charge at the wall, and the secondary electro-osmotic flows (or electro-osmotic recirculating rolls) contributed by the field-effect-induced surface charge act as the perturbed flow. By time-periodic switching two different secondary electro-osmotic flows, it makes streamlines to cross at successive intervals and results in chaotic mixing. Dynamic system techniques such as Poincaré map and finite-time Lyapunov exponent analyses are employed to describe the behaviors of particle motion in this mixing system. Finally, the optimum operating condition (e.g. amplitude and time-switching period) for the mixing is identified.

Introduction

Recently, micro-scale devices have been proposed as a means of constructing micro-total analysis systems (μ-TAS) or Lab-on-a-Chip (LOC) devices. These devices have received much attention in a variety of chemical and biological applications [1]. Mixing of different reactants is an important process for most biochemical applications such as polymer chain reaction (PCR) and DNA hybridization. In convectional laboratories, mixing is usually performed by either manually shaking the test tube or mixing using a stirrer. Unfortunately, these convectional mixing methods are difficult to implement in miniaturized systems. Therefore, developing novel methods for rapid and efficient mixing is crucial for the development of μ-TAS.

In large-scale devices, turbulent enhancement has been an effective method to achieve efficient mixing. However, it is much more difficult to induce turbulence in micro-scale devices due to the viscous forces dominate the flow at low Reynolds number. Laminar mixing through molecular diffusion usually is too slow for most practical applications. Therefore, the development of micro-mixing approaches for microfluidic applications has attracted the attention of many research groups worldwide, and a quite large number of micro-mixers based on different strategies have been proposed [2]. In particular, mixing by chaotic advection is considered to be one of the most promising approaches for rapid and efficient mixing in laminar flows [3]. In chaotic advection, fluid elements always are stretched and folded repeatedly. It provides an effective increase in the interfacial contact area and con-

[1]Department of Engineering Science, National Cheng Kung University E-mail: rjyang@mail.ncku.edu.tw

centration gradient due to the reduction of striation thickness (i.e. diffusion length). In this way, the mixing time and length can be considerably reduced.

In this study, we propose a novel technique to create chaotic mixing in low Reynolds number electro-osmotic flows. Electro-osmotic flow refers to the movement of bulk liquid relative to a stationary charged surface (e.g. microchannel) under an externally applied electric field. Electro-osmotic flow has became a popular means to drive flow in microfluidic devices in recent years [4], which do not involve mechanical moving parts and are readily integrated within microfluidic devices using standard micro-fabrication methods. In the mixing system (see Figure 1), the plug-like electro-osmotic flow is a throughput flow contributed by the permanent zeta potential of the microchannel, and time-wise periodic alternating secondary electro-osmotic (SEO) flows (or electro-osmotic recirculating rolls) contributed by the field-effect-induced zeta potential act as the perturbed flow. Chaotic mixing occurs when appropriate operating conditions (e.g. amplitude of perturbation and frequency) are applied. Several techniques such as Poincaré map, finite-time Lyapunov exponent, and back-trace imaging analyses are used to examine the existence of chaos and evaluate the mixing performance of this mixing system.

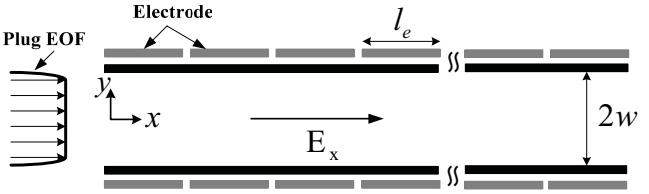

Figure 1: Schematic illustration of electro-osmotic flow mixing in a microchannel with spatiotemporal zeta potential modulation using the field-effect control.

Mathematical model

Governing equation

We consider mixing in a microchannel with high aspect ratio (i.e., channel height is much larger than channel width) in our work. The two-dimensional flow is assumed. Furthermore, the Reynolds number usually is much smaller than unity in electro-osmotic flows, and the flow can be modeled with Stokes equation. Due to the time-switching period of two different SEO flows is much larger than three time scales: (1) the charge relaxation time of electrical double layer (EDL) capacitor, (2) time required for fully charging the capacitor of the wall (field-effect), and (3) viscous diffusion time of fluid in this study, the time-dependent flow can be regarded as quasi-steady Stokes flow [5]. With the thin double layer assumption, the Helmholtz-Smoluchowski slip boundary condition is considered as the electro-osmotic effect. Consequently, the flow can be described by the following

bi-harmonic equation:

$$\nabla^4 \Psi = 0 \tag{1}$$

where Ψ is the dimensionless stream function. The dimensionless velocity field can be represented by $\{U,V\} = \{\partial\Psi/\partial Y, -\partial\Psi/\partial X\}$. Equation (1) can be easily solved by separation of variables and series expansion. The secondary electro-osmotic flow fields corresponding to three different spatial field-effect-induced zeta potential distributions are shown in Figure 2, respectively.

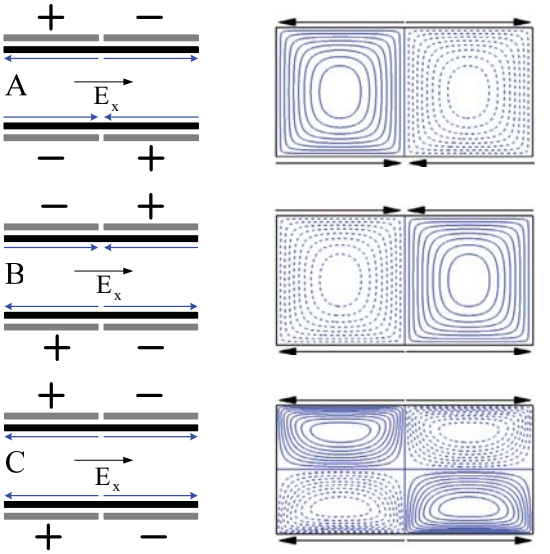

Figure 2: Secondary electro-osmotic flow patterns resulting from three different spatial field-effect-induced zeta potential distributions.

Kinematic model for the mixing system

The equation for the motion of advected passive particle in Largangian representation is given below:

$$\frac{d\mathbf{X}}{d\tau} = \mathbf{U}_A(X,Y)\, g_A(\tau) + \mathbf{U}_{\text{B or C}}(X,Y)\, g_{\text{B or C}}(\tau) \tag{2}$$

where

$$g_A(\tau) = \begin{cases} 1, & (k-1)T < \tau < (2k-1)T/2 \\ 0, & (2k-1)T/2 < \tau < kT \end{cases}$$

$$g_{\text{B or C}}(\tau) = \begin{cases} 0, & (k-1)T < \tau < (2k-1)T/2 \\ 1, & (2k-1)T/2 < \tau < kT \end{cases}$$

$\mathbf{X}$ is the location of the advected passive particle, the dimensionless time $\tau = tu_o/w$, the dimensionless time period $T = T^* u_o/w$, and the number of time periods $k = 1, 2, 3.....$ Note that $\mathbf{U}_A$, $\mathbf{U}_B$, and $\mathbf{U}_C$ represent the total velocity fields of plug-like electro-osmotic flow and secondary electro-osmotic flow for three different spatial zeta potential modulations, respectively. Two different temporal zeta potential modulations are considered to explore the chaotic advection in electro-osmotic flows. One is the time-wise alternation of flow patterns A and B (namely Design I mixing system), and another is the alternation of flow patterns A and C (namely Design II mixing system).

Results

Poincaré map analysis

The Poincaré maps for Design I and Design II are shown in Figures 3 and 4, respectively. The lines represent the particles move in periodic manners. These lines are termed as Kolmogorov-Arnold-Mose (KAM) curves or boundaries [3]. The white region is isolated due to the presence of KAM curve. It could be an ordered area, or it could contain both ordered and chaotic areas. Any trajectory of a point initiated in one attractor (periodic area or chaotic area) cannot cross over the KAM curves to another attractor. In other words, the KAM curves act as boundaries that prevent the mixing of material elements between the two separated areas without considering the molecular diffusion effect. In Design I (Figure 3), it can be seen that KAM boundaries are significant at any time period (T), which implies poor mixing when molecular diffusion effect is insignificant. From Poincaré maps analysis, the better time periods for mixing in Design I are $T = 3.5$and $T = 4.0$due to the smaller white region (unmixed region). From Figure 4, it can be seen clearly that KAM boundaries or unmixed regions are not significant compared to Figure 3 expect the cases of $T = 1.0$ and $T = 2.0$. When $T = 3.5$, $T = 4.0$, $T = 4.5$, $T = 5.0$, and $T = 8.0$, the results indicate that the particles move in more chaotic behaviors. The system seems nearly fully chaotic under these operating conditions. This also implies the better choice of time period for mixing among them, but an optimal time period for the mixing has undecided yet.

Finite-time Laypunov exponent analysis

Lyapunov exponent refers to the average exponential rates of divergence or convergence of nearby orbits in the phase space. In other words, Lyapunov exponent can describe the stretching rates of material elements in a quantitative manner. The Lyapunov exponent is expressed as Equation (3), which is given by

$$\lambda(\tau) = \lim_{|d\mathbf{X}_0| \to 0} \frac{1}{\tau} \ln \left[\frac{|d\mathbf{X}(\tau)|}{|d\mathbf{X}_0|} \right] \tag{3}$$

where $|d\mathbf{X}_0|$ and $|d\mathbf{X}(\tau)|$ are the distance between two particles at initial condi-

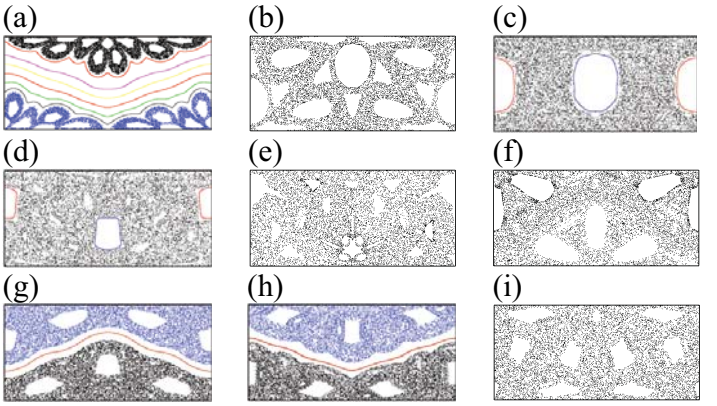

Figure 3: Poincaré maps for the different time periods when $A_p = 2.0$and$L_e = 2.0$in Design I (a)$T = 1.0$, (b)$T = 2.5$, (c)$T = 3.0$, (d)$T = 3.5$, (e$T = 4.0$, (f)$T = 4.5$, (g)$T = 5.0$, (h)$T = 7.0$, and (i)$T = 8.0$. Note $A_p$is the amplitude of perturbed flow defined as the Smoluchowski velocity ratio of secondary EO to plug-like EO.

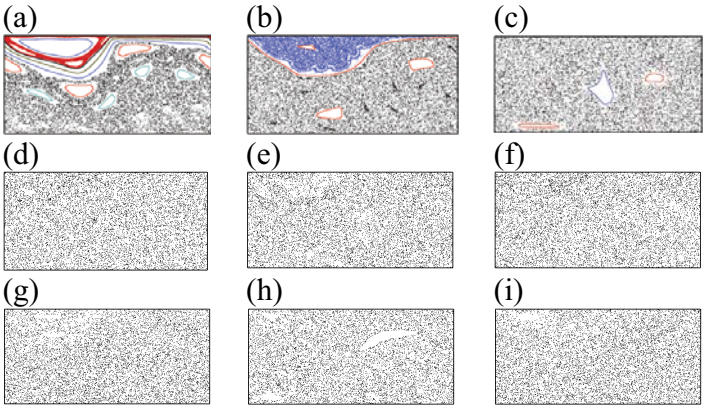

Figure 4: Poincaré maps for the different time periods when $A_p = 2.0$and$L_e = 2.0$in Design II (a)$T = 1.0$, (b)$T = 2.0$, (c)$T = 3.0$, (d)$T = 3.5$, (e$T = 4.0$, (f)$T = 4.5$, (g)$T = 5.0$, (h)$T = 7.0$, and (i)$T = 8.0$.

tion and time τ, respectively. This study adopts Sprott's method to calculate the value of the Lyapunov exponent (i.e. largest Lyapunov exponent). When $\tau \to \infty$, Lyapunov exponent converges to a value termed as infinite-time Lyapunov exponent. The calculation of infinite-time LE usually is a time-consuming work. In a fully chaotic system, infinite-time LE is not dependent on the initial positions of particles. Due to the mixing system may not be fully chaotic (see Figures 3 and 4), the choice of initial positions to calculate infinite-time LEs of different attractors is

difficult. In addition, infinite-time LE is not a practical mixing index because the complete mixing within a short mixing time is usually required in practical applications. Finite-time LE may be a more practical mixing index than infinite-time LE. Unlike infinite-time LE, Finite-time LE is dependent on the initial position of particle and time. The domain of one period unit of mixing channel was divided into uniform grids ($\Delta X = 0.025$ and $\Delta Y = 0.025$), which are used as initial points to calculate FTLEs. The mean FTLE of $\tau = 100$ as a function of time period at different amplitudes for Designs I and II are shown in Figure 5. The results indicate that the mean FTLE increases significantly as the amplitude increases in Design II. It also reveals the mixing performance in Design II is better than Design I due to larger FTLE implies larger stretching rate of material element. The better operating time period in Design II seems is between 3.0 and 5.0 for any amplitude. $T = 4.0$seems to be the optimal time period at the amplitude $A_p = 2.0$in Design II.

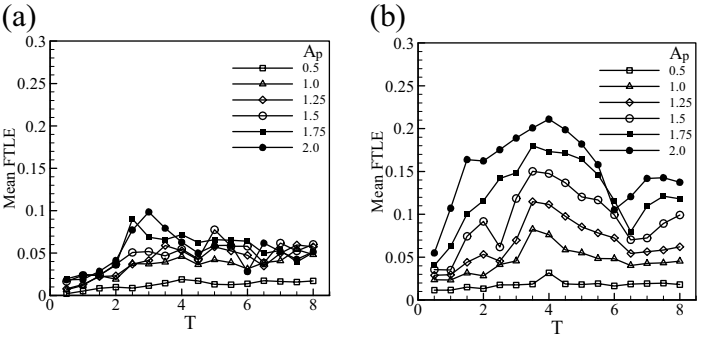

Figure 5: Mean FTLE ($\bar{\lambda}$) in terms of time period (T) at different amplitudes of perturbation source (A_p) for different mixing systems. (a) Design I and (b) Design II.

The mean FTLE may not be an appropriate mixing index to evaluate the mixing performance because the system may consist of low and high FTLE regions. The uniformity of FTLE distribution should also be considered to evaluate the mixing performance, i.e. the statistic of FTLE distribution is necessary. Figures 6 and 7 show the FTLE distribution within one period unit of mixing channel at different amplitudes in Design I and Design II, respectively. The results show the white regions shown in Figures 3 and 4 are approximately zero FTLE, i.e. zero stretching rate. The statistical value: mean value, standard deviation (σ), coefficient of variance (CV) for FTLE distribution are also shown in Figures 6 and 7. The value of CV is used as a mixing index to evaluate the mixing performance. The smaller CV implies the better mixing. The optimal time period for mixing is $T = 3.5$at $A_p = 2.0$.

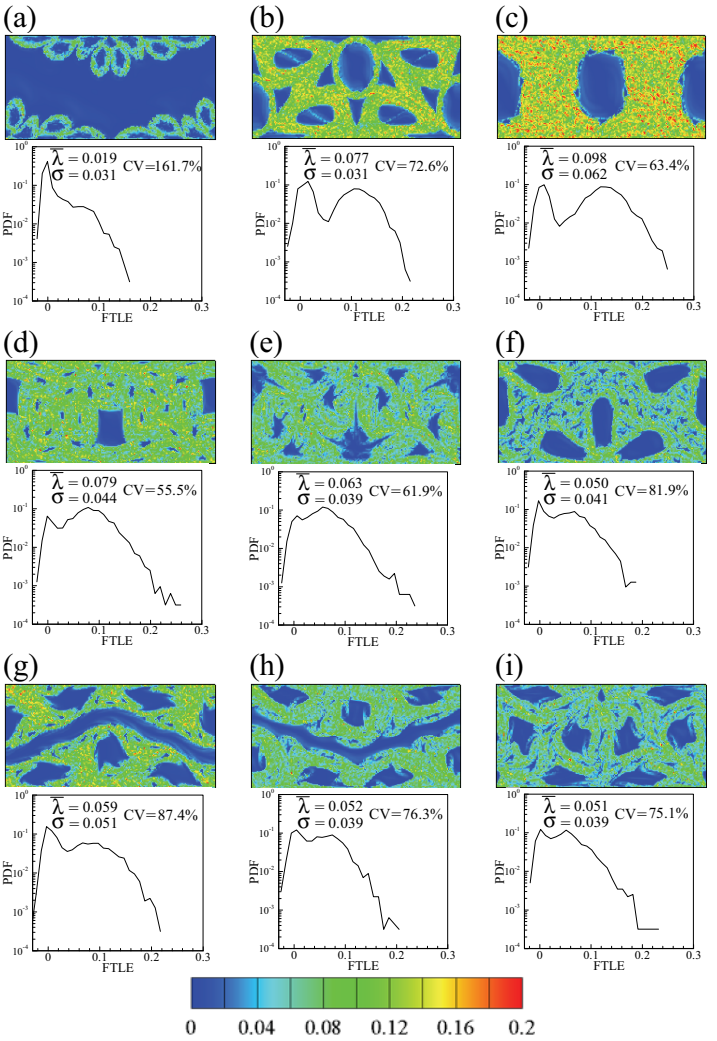

Figure 6: Contour plots of FTLE distribution and probability density functions (PDF) of FTLE for the different time periods when $A_p = 2.0$and$L_e = 2.0$in Design I (a)$T = 1.0$, (b)$T = 2.5$, (c)$T = 3.0$, (d)$T = 3.5$, (e$T = 4.0$, (f)$T = 4.5$, (g)$T = 5.0$, (h)$T = 7.0$, and (i)$T = 8.0$. Note that $\sigma$and CV are standard deviation and coefficient of variance ($\sigma/\bar{\lambda} \times 100\%$), respectively.

Visualization of mixing

We adopt back-trace imaging method to visualize mixing. At $\tau \approx 40$, the mixing images for Designs I and II at different time-switching periods are shown in Figures 8 and 9, respectively. It can be seen obviously that the mixing in Design II is better than Design I. It is consistent with the result from Poincaré map and FTLE

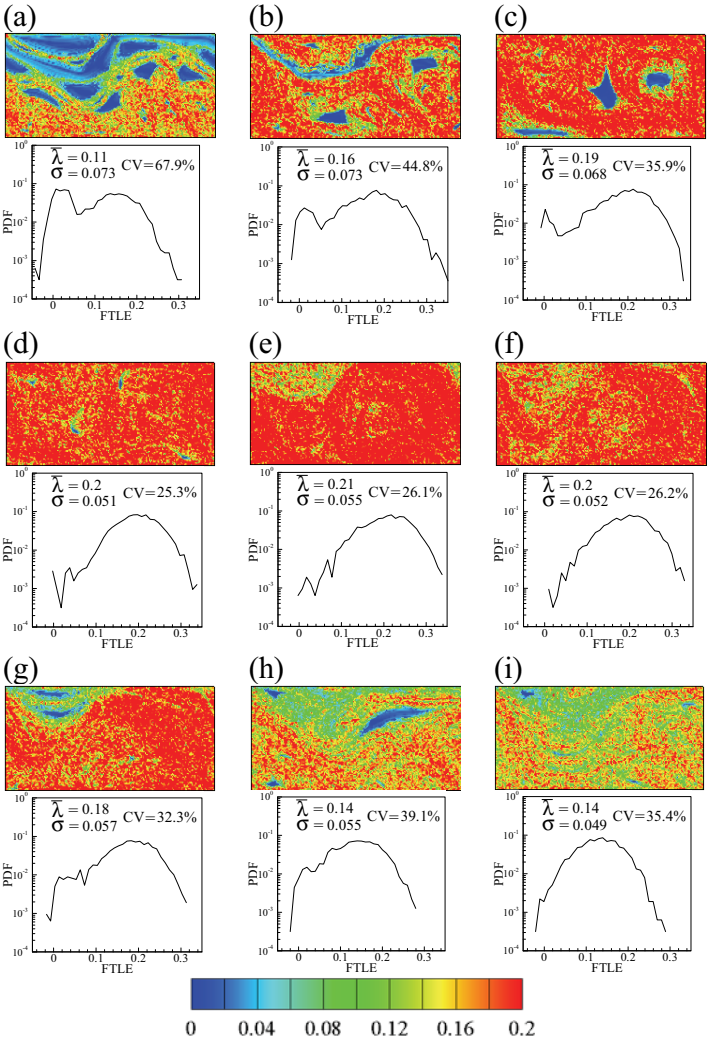

Figure 7: Contour plots of FTLE distribution and probability density functions (PDF) of FTLE for the different time periods when $A_p = 2.0$and$L_e = 2.0$in Design II (a)$T = 1.0$, (b)$T = 2.0$, (c)$T = 3.0$, (d)$T = 3.5$, (e$T = 4.0$, (f)$T = 4.5$, (g)$T = 5.0$, (h)$T = 7.0$, and (i)$T = 8.0$.

analyses. The poor mixing regions shown in Figure 9 are consistent with the low FTLE value regions shown in Figure 7. The best time-switching period for mixing is $T = 3.5$.

Conclusion

The Poincaré map and finite-time Lyapunov exponent analyses both have been

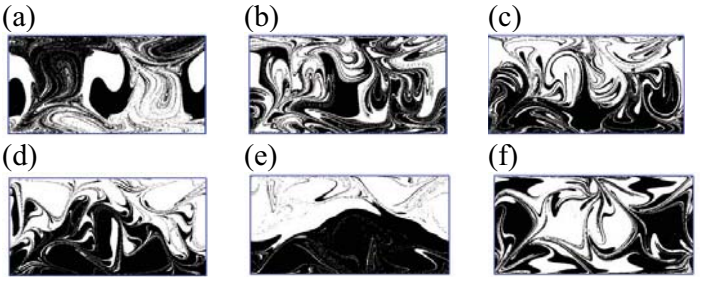

Figure 8: Mixing images for different time periods when $A_p = 2.0$and$L_e = 2.0$in Design I. (a)$T = 3.0$, (b)$T = 3.5$, (c)$T = 4.0$, (d)$T = 4.5$, (e)$T = 5.0$, (f)$T = 8.0$.

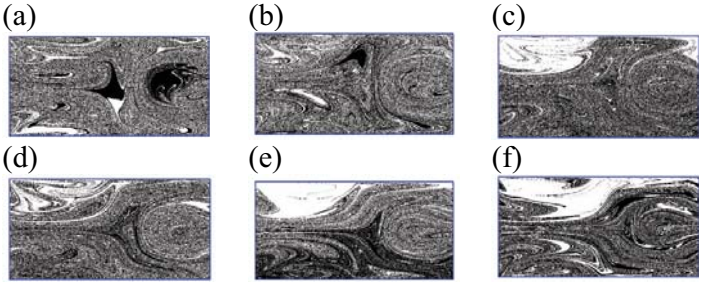

Figure 9: Mixing images for different time periods when $A_p = 2.0$and$L_e = 2.0$in Design II. (a)$T = 3.0$, (b)$T = 3.5$, (c)$T = 4.0$, (d)$T = 4.5$, (e)$T = 5.0$, (f)$T = 8.0$.

employed to investigate the chaotic mixing. The coefficient of variance for FTLE distribution was used as a mixing index to evaluate the mixing performance. $T = 3.5$was identified to be the optimal time period for mixing at the amplitude 2.0 in both Design I and Design II. The mixing performance of Design II is better than that of Design I.

Acknowledgement

The work was supported in part by the National Science Council of Taiwan under Grant No. NSC-96-2628-E-006-162-MY3.

References

1. Stone HA, Stroock AD, and Ajdari A. Engineering flows in small devices: microfluidics toward a lab-on-a-chip. *Annu. Rev. Fluid Mech.* **36**, 381-411, 2004.
2. Chang C-C and Yang R-J. Electrokinetic mixing in microfluidic systems. *Microfluid. Nanofluid.* **3**, 501-525, 2007.
3. Ottino JM. *The Kinematics of Mixing: Stretching, Chaos, and Transport*. Cambridge University Press, 1989.

4. Chang H-C. Electro-kinetics: A viable micro-fluidic platform for miniature diagnostic kits. *Can. J. Chem. Eng.* **84**, 146-160, 2006.
5. Chang C-C and Yang R-J. Chaotic mixing in a microchannel utilizing periodically switching electro-osmotic recirculating rolls. *Phys. Rev. E* **77,** 056311.